

BINARY IMAGE SKELETON

Continuous Approach

Leonid Mestetskiy

Department of Mathematical Methods of Forecasting, Moscow State University, Moscow, Russia

Andrey Semenov

Department of Information Technologies, Tver State University, Tver, Russia

Keywords: Binary image, continuous skeleton, discrete skeleton, polygonal figure, pruning, skeletal base.

Abstract: In this paper we propose a building technique of a correct model of continuous skeleton for discrete binary image. Our approach is based on approximation of each connected object in an image by a polygonal figure. Figure boundary consists of closed paths of minimal perimeter which separate points of foreground and background. Figure skeleton is constructed as a locus of centers of maximal inscribed circles. In order to build a so-called skeletal base from figure skeleton, we cut unnecessary noise from it. It is shown, that the constructed continuous skeleton exists and is unique for each binary image. This continuous skeleton has the following advantages: it has a strict mathematical description, it is stable to noise, and it also has broad capabilities of form transformations and shape comparison of objects. The proposed approach gives a substantial advantage in the speed of skeleton construction in comparison with various discrete methods, including those in which parallel calculations are used. This advantage is demonstrated on real images of big size.

1 INTRODUCTION

Mathematical concept of a skeleton has been formulated initially only for continuous objects (Blum, 1967). A skeleton of a closed region on Euclidean plane is defined as a set of centers of maximal empty disks. A disk is empty if each internal point of it is also internal point of the region. In order to use the concept of a skeleton as a research tool of image shape in digital images, one needs to extend this concept to discrete space. However, in spite of seeming simplicity, it is not possible to extend this definition to discrete images immediately (Smith, 1987; Ogniewicz and Kubler, 1995; Bai et al., 2007). Efficient algorithms of continuous skeleton construction are known only for polygonal regions (Lee, 1982; Fortune, 1987; Yap, 1987; Klein and Lingas, 1995). However, for exact polygonal approximation of discrete form boundaries, one needs to use many small rectilinear segments. This leads to an increase in the number of vertices of approximating polygons. But the more vertices there are in polygons, the more noisy

branches of skeleton are generated. And these branches are not important for an analysis of image shape.

Since it is impossible to use continuous skeleton for image analysis, «discrete skeleton», an analogue of continuous skeleton, is constructed for these purposes. A discrete skeleton is usually defined as a binary image derived by a certain transformation of the initial image. The skeleton consists of pixel-wide lines and all of these lines are approximately equidistance from the boundary of the initial object. There exist several approaches of construction of such transformation: topological thinning, morphological erosion and allocation from a distance map (Costa and Cesar, 2001). However, discrete skeletons obtained by these methods have essential disadvantages in comparison with their continuous analogues. In methods of topological thinning and morphological erosion the Euclidian metric is lost. Skeletonization methods by distance map cause loss of skeleton connection. In addition presentation of skeletons as binary images complicates their comparison. It is also impossible

to transform image shape on the basis of a discrete skeleton.

Another approach, proposed in (Ogniewicz and Kubler, 1995), uses a subgraph of the Voronoi diagram of object boundary points as a skeleton of a discrete object (Fig.1(a-d)). This subgraph is extracted from the Voronoi diagram on basis of regularization procedure. Therefore, the resulting continuous skeleton is a planar linear graph. Since it is continuous and not discrete, it suits much better for image shape transformation and comparison. The disadvantage of the resulting skeleton is that its branches are often zigzag. This disadvantage becomes especially pronounced for images of low resolution (Fig.1(d)). In addition, when this method is applied to a complex image of high resolution, which also has regular elements (for example, to a drawing with rectilinear fragments), a big number of "redundant" boundary pixels becomes involved in processing, which leads to an unnecessary increase in the dimension of Voronoi diagram and the total amount of calculations.

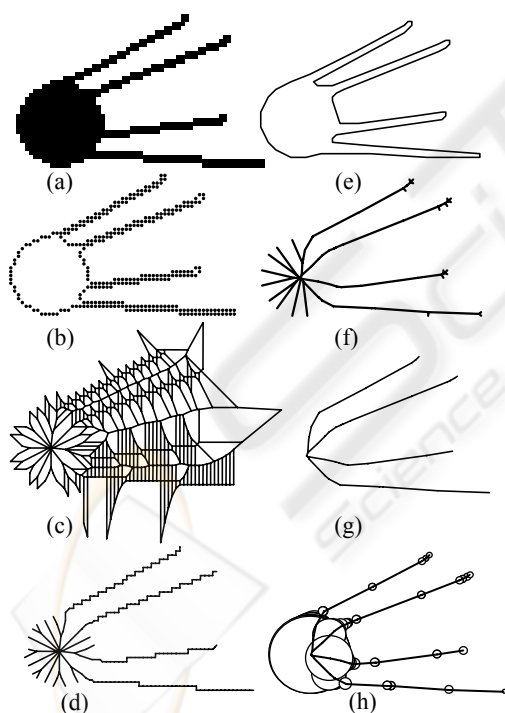


Figure 1: (a) – the binary image, (b) – the boundary points, (c) – the Voronoi diagram of boundary points (only finite edges), (d) – regularization of the Voronoi diagram, (e) – the approximating polygonal figure, (f) – the figure skeleton, (g) – the skeleton regularization, (h) – the radius function of skeleton.

Not only the quality of a skeleton constructed by a specific algorithm is important. The speed with which this algorithm works is very important in computer vision systems. Currently speed enhancement is usually achieved by the development algorithms of parallel discrete skeletonization (Manzanera et al., 1999; Deng et al., 2000; Strzodka and Telea, 2004). However this acceleration has its limits since there remain sequential steps in discrete skeleton construction algorithms and the number of these steps increases with the growth of image size. Image size, in turn, increases steadily as resolution of cameras and scanners increases.

In reality, the time necessary for skeletonization of big images even on modern computers is still too big for many applications.

Therefore, the issue of extension of the concept of continuous skeletons on discrete images seems far from being resolved. The purpose of this paper is to describe a continuous approach to skeletonization of binary images (Fig.1(e-h)) developed by the authors and its application to real-world problems (Mestetskiy, 1998, 2000, 2006). The advantages of the proposed method are also demonstrated in the paper. The main advantages include superiority in computer efficiency.

2 DISCRETE FIGURE AND ITS SKELETON

We will define a skeleton of a discrete image on the basis of the following concepts:

- a discrete figure;
- an approximating minimal perimeter polygonal figure;
- a continuous skeleton of a polygonal figure;
- a skeletal base of a polygonal figure.

2.1 Discrete Figures in Binary Image

A binary image is a two-colored picture where one or several objects of one color are located on a background, which has another color. Without loss of generality, we will consider a binary image as a black-and-white image: object is black, and background is white. Such image is represented in a computer as a matrix of black and white pixels.

Let us define an adjacency structure on a set of pixels as follows. For a black pair of pixels we will define neighborhood as 8-adjacency, and for a white pair and a two-colored pair – as 4-adjacency.

A set of one-colored pixels is called connected if for each pair of pixels in it there is a path from one pixel to another, consisting of sequentially neighboring pixels of the same color. Maximal connected set of pixels of one color is called a connected component. If all pixels of a component lie on the same straight line, such a component is called degenerated. Let us define discrete figures as connected black-colored components. There are 5 connected components in the image in Fig.2(a), two of them are discrete figures.

2.2 The Continuous Approximation of Discrete Figure

Let us regard pixels as points with integer coordinates on Euclidean plane.

We will call a pair of 4-adjacent two-colored points a boundary pair, a segment connecting these points – a boundary segment. Two components to which points of a boundary pair belong are called adjacent, and the boundary pair is called dividing for these components. The set of all dividing boundary pairs for two adjacent components we will name a boundary corridor (Fig.2(b)). Each discrete figure defines one or more boundary corridors.

Let us say, that a closed path lies in a boundary corridor if it crosses all boundary segments of this corridor. We will consider that a path crosses a segment if it has a common point with it and lies on different sides from this segment in some neighborhood of the intersection point. There will exist a minimal length path in the set of paths lying in a boundary corridor. This path will be a closed polyline and we will call it a separating minimal perimeter polygon (MPP). If a discrete figure and all its holes are not degenerated then all its MPP are simple polygons (Fig.2(c)). For a degenerated figure or a degenerated hole MPP degenerates in a line segment. The set of all MPP of a discrete figure defines a polygonal figure – «a polygon with polygonal holes».

Thus, we have defined minimal perimeter polygonal figures that approximate discrete figures of binary image. It is important to note that the set of approximating polygonal figures always exists and is unique for a given binary image.

2.3 Polygonal Figure Skeleton

Degenerated disks of zero radiuses centered in the convex vertices of a polygonal figure are empty as they have no internal points and, therefore, don't contain boundary points of a figure. Besides, they

are the maximal empty disks since they don't contain other empty disks. Therefore points, which coincide with convex vertices of a polygonal figure, belong to a polygonal figure skeleton.

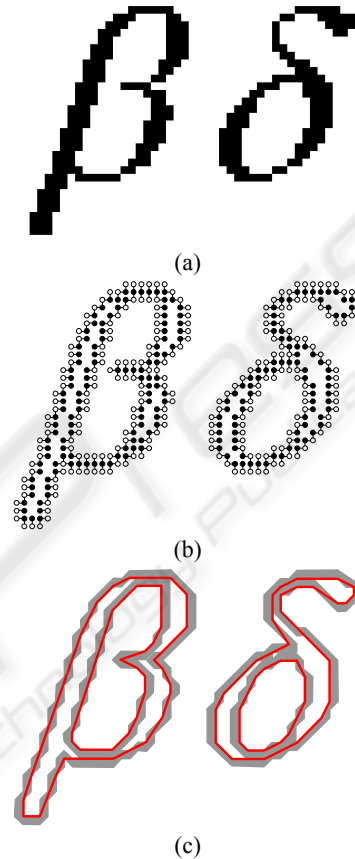


Figure 2: (a) – the binary image with 5 components and 2 discrete regions, (b) – boundary corridors, (c) – minimal perimeter polygons.

A polygonal figure skeleton is a planar graph with edges consisting of line segments and parabolas (Lee, 1982). The vertices of this skeleton are comprised from the convex vertices of a polygonal figure (one degree vertices) and from the points, which are centres of the inscribed circles, tangent to figure boundary in three or more points (three and more degree vertices). The radial function is defined in each skeleton point as the radius of an inscribed circle centered in this point.

It is important to underline that a polygonal figure skeleton always exists and is unique.

2.4 Polygonal Figure Skeletal Base

The problem of “noise” branches exists for both continuous and discrete skeletons. Small

irregularities in figure boundary lead to occurrence of skeleton branches, unessential for analysis of image form. The task of skeleton regularization is to remove these branches and leave only fundamental part of the skeleton which at the same time characterizes properties of the shape. This fundamental part looks like a skeleton subgraph. We will name it a skeletal base. Since the transformation of a skeleton into a skeletal base is achieved by the removal of unessential vertices and edges, this process is called *pruning*.

Let C be a polygonal figure. Let us call its boundary ∂C , its skeleton – S and its skeleton radial function – $\rho(s)$, $s \in S$. The skeleton will be a planar graph $S = (P, E)$ with the set of vertices P and edges E . We will call a skeleton vertex with one incident edge terminal, and with two or more edges – internal. An edge incident to a terminal vertex is also called terminal; an edge incident to two internal vertices is called linking. Linking edges can enter in one or more cycles and in this case they are called cyclic.

Pruning is a consecutive removal of some terminal vertices and skeleton edges incidental to them. In the process of pruning, degree of some vertices changes. In particular, internal vertex can become terminal or its degree can become 2.

Pruning guarantees preservation of skeleton connectivity and also preservation of all cycles in a skeleton as it doesn't touch cyclic edges.

Let us consider an assessment criterion of "essentiality" of a terminal edge. Essential edges remain in a skeletal base, and unessential edges are cut.

Let $S' = (P', E')$ be some adjacent subgraph of a skeleton $S = (P, E)$, such that $P' \subseteq P$, $E' \subseteq E$ and also such that in the set $E \setminus E'$ there are no cyclic edges of skeleton. This means, that graph S' can be obtained from skeleton S by the removal ("pruning") of some vertices and edges of skeleton, and such removal doesn't destroy cycles and doesn't break connectivity of the graph. This graph S' we will call *truncated* subgraph of S . We will consider the set of points formed by union of all inscribed circles, centered in points of the truncated subgraph S' , whose radiuses are equal $\rho(s)$, $s \in S'$. This set of points forms a closed region which we will call a silhouette of subgraph S' . The important property of a truncated subgraph silhouette is its topological equivalence to figure C . In particular, a silhouette is a connected set.

Let a skeletal base of figure C be the minimal truncated subgraph S' of its skeleton S with silhouette $V_{S'}$ satisfying a condition $H(C, V_{S'}) \leq \varepsilon$, where $\varepsilon > 0$ is a regularizing parameter, and $H(C, V_{S'})$ – Hausdorff distance between figure C and silhouette $V_{S'}$.

It is necessary to note, that for each value of parameter ε the skeletal base always exists and is unique.

We will call the derived skeletal base a continuous skeleton of a discrete figure.

3 ALGORITHMS

3.1 Boundary Corridor

The construction of a boundary corridor consists of two stages: the corridor search and its tracing. Corridor search is understood as a problem of finding one boundary pair of points (Fig.3(a)). Search of such pair can be executed by row scanning of the binary image. After finding the boundary pair, the boundary tracing algorithm will work. This algorithm reveals all other boundary pairs of a corridor. After corridor tracing is finished, the algorithm starts the search of next corridor from that location where the first boundary pair of the previous corridor has been found. The process ends, when the single line scanning ends.

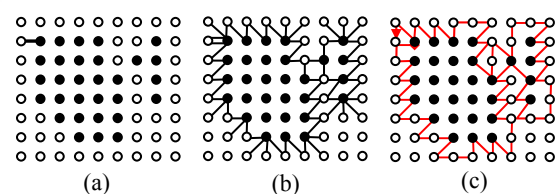


Figure 3: Corridor tracing: (a) the initial position of tracer pair, (b) the consecutive positions of tracer pair, (c) the sequence of test points (tracing track).

The algorithm starts contour tracing from the first boundary pair and finds sequentially other boundary pairs of a corridor. A boundary pair of points currently found by the algorithm we will call a tracer pair. Tracing process corresponds to the consecutive movement of the white end of the tracer pair in a positive direction relative to the black end (Fig.4). The derived point is called a test point. All possible variants of test point choice at different positions of the tracer pair are presented on Fig.4.

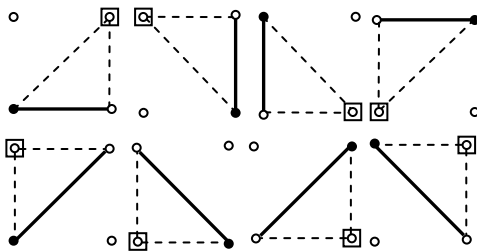


Figure 4: Choice of the next test point (labeled as square) for different positions of tracer pair (solid line) during tracing process of boundary corridor.

Current position of the tracer pair is shown by a solid line, and new possible positions depending on color of a test point – by a dotted line.

A new position of a tracer pair is determined from the color of a test point by the following rule. The test point replaces in the tracer pair a point of the same color as it is.

Consecutive moving of a tracer pair allows to single out all boundary points corresponding to one boundary contour (Fig.3). Tracing process ends when tracer pair will return to its initial position.

3.2 Minimal Perimeter Polygon

The sequence of test points forms an ordered list called a tracing track (Fig.3(c)). We will attain "walls" of a boundary corridor by sequentially connecting all black points of this list among themselves and all white points. The left wall consists of black points, and the right one – of white points. The minimal perimeter polygon lies between the corridor walls. All vertices of MPP are points of a tracing track. We will call such points a corner. The task of MPP construction is to choose corner points from a tracing track.

The first corner point is defined from the initial position of the tracer pair (Fig.3(a)). It is obvious, that the right point of this pair is always corner. Let us note, that the two consecutive vertices in MPP should be connected by line segment lying between corridor walls completely. It means, that if another (in particular, the first) corner point is found, it is necessary to search for the next corner point as for a point lying from it «in the line of sight» inside a corridor.

Let us define a concept of a «coverage sector» for a corner point. At the initial moment (for the current found corner point) it equals 360° and isn't limited by anything. As the algorithm proceeds, the points of the track after this corner point are

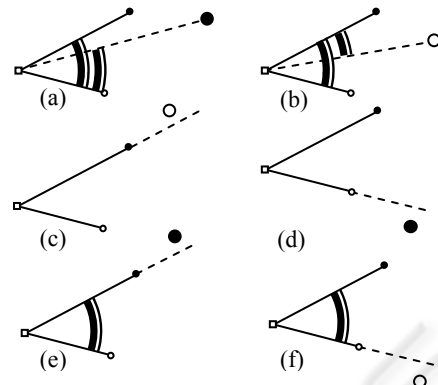


Figure 5: (a,b) correction of coverage sector, (c,d) new angular point forming, (e,f) coverage sector doesn't change.

sequentially considered and the coverage sector is modified by following rules (Fig.5):

1. If the test point is located inside the coverage sector, the sector changes (Fig.5(a,b)). If the test point is black (Fig.5(a)), it is declared as the left side of the sector, if it is white (Fig.5(b)) – as the right one.
2. If the white point is located outside the coverage sector to the left of its left side (Fig.5(c)), the left black point of the sector is declared the new corner point. Similarly, if the black point is located outside the sector to the right of its right side (Fig.5(d)), the right white point is declared the new corner point.
3. In all other cases (Fig.5(e,f)) the coverage sector doesn't change.

As these rules are followed, all corner points are sequentially found. In the process, the corridor track is regarded as a circular list of points. The process ends when the initial corner point is chosen as a new corner point (but not as a test point!) once again.

3.3 The Construction of Skeletons

Fast algorithms for skeleton construction of simple polygons with n vertices have computational complexity $O(n \log n)$ (Lee, 1982) and $O(n)$ (Klein and Lingas, 1995). Known generalizations to the case of a polygonal figure with holes (Srinivasan et al., 1992, Lagnon and Sobolev, 2001) have computational complexity $O(kn + n \log n)$, where k is the number of polygonal holes and n is the general number of vertices. For some problems such computational complexity takes too much. For example, in the task of construction of an external skeleton for segmentation of the text document

image (Mestetskiy, 2006) values k and n have an order 10^3 and 10^5 accordingly. At the same time, efficient algorithms for Voronoi diagram construction of linear segment set (Fortune, 1987; Yap, 1987) don't use specific features of segment set of polygonal figure boundary because of their universality. In particular, these algorithms build Voronoi partitioning not only inside, but also outside of a polygonal figure and this is superfluous work.

Our solution is based on the concept of adjacency of polygonal figure boundary contours and on the construction of so-called adjacency tree of these contours.

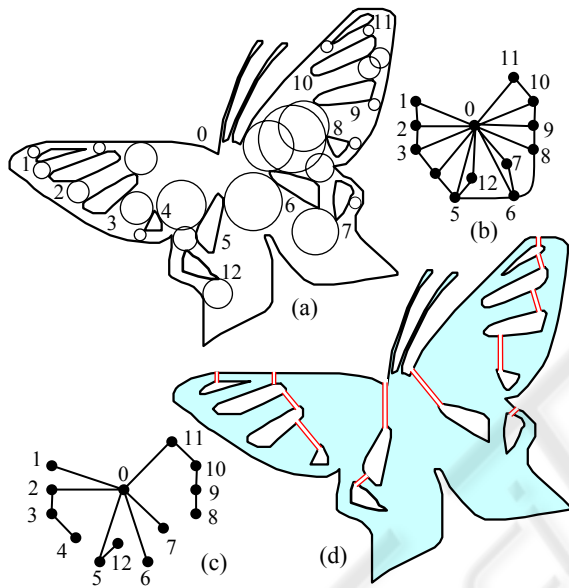


Figure 6: Figure boundary adjacency tree construction: (a) the polygonal figure and intercontour circles, (b) the boundary adjacency graph, (c) the boundary adjacency tree, (d) transforming of the figure to the polygon.

Two boundary polygons are adjacent if the circle inscribed into a figure, which contacts both of these polygons exist. The given relation of contour adjacency defines a graph of contour adjacency. It is obvious, that this graph is connected. Each spanning set of it (the minimal connected spanning subgraph) is a tree. Such tree we will call a polygonal figure boundary adjacency tree. In figure 6a the image with 12 boundary contours is presented. Inscribed circles, contacting pairs of contours, show the adjacency relation. In Fig.6(b) the polygonal figure boundary adjacency is shown, and in Fig.6(c) one of the boundary adjacency trees is presented.

The boundary adjacency tree gives the chance to reduce a problem of a polygonal figure skeletonization to a problem of a simple polygon

skeletonization. For this purpose let us transform chains of polygon sides into one chain by «cutting-in» them into one another. As a result the polygonal figure conditionally transforms to "polygon" (Fig.6(d)). An $O(n \log n)$ swepline algorithm for boundary adjacency tree finding and figure skeleton construction is described in (Mestetskiy, 2006).

3.4 Skeletal Base

It is possible to present the process of a skeletal base construction as a construction of a sequence of truncated subgraphs of skeleton $\{S'_m\}$. Here $S'_0 = S$, $S'_{m+1} \subset S'_m$, $m=0, \dots, M$, and for all S'_m the following condition is satisfied: $H(C, V_{S'_m}) \leq \epsilon$. The last element of this sequence S'_M is the required skeletal base. According to our definition of a skeletal base, for each truncated subgraph $S' \subset S'_M$ condition $H(C, V_{S'}) > \epsilon$ takes place or there are no terminal edges in S'_M . The described process is illustrated by an example in Fig.7. Here $\epsilon = 2$.

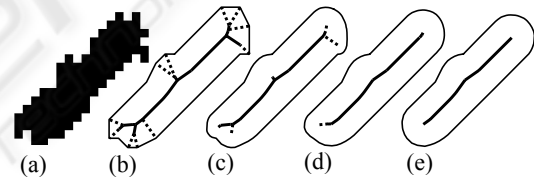


Figure 7: Skeletal base construction: (a) the initial image, (b) the polygonal figure and its skeleton, (c,d,e) the skeleton subgraphs and their silhouettes.

Computational complexity of this algorithm depends on the number of skeleton vertices linearly, i.e. it is at worst $O(n)$, where n is the number of polygonal figure vertices.

4 EXPERIMENTS

The described method of continuous skeleton construction of a binary image has been implemented and has passed multiple checks in different applications.

Theoretical estimates of computational complexity of algorithms, with all their importance, don't give full conception about the possible application of algorithms in computer vision systems. Therefore there is a necessity to perform

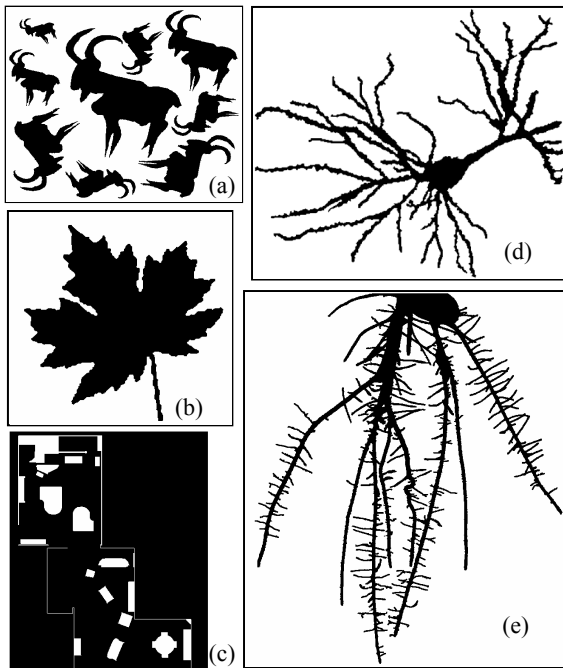


Figure 8: Test examples: (a) Billygoat, (b) leaf1, (c) room, (d) neuron, (e) roots.

experimental estimates based on real working algorithms and on practical examples. There is not many publications describing such experiments. Usually there is no information about software implementation and algorithm running time at all (Manzanera et al., 1999) or there are only results of computing experiments with "toy" examples of very simple images (Deng et al., 2000).

The most difficult examples (Fig.8) of images and real time expenses for their skeletonization are presented in works (Ogniewicz and Kubler, 1995; Strzodka and Telea, 2004).

Table 1: Comparison of our algorithm CS and algorithm OK (Ogniewicz and Kubler, 1995).

	OK	CS	OK/CS
sites	11104	1874	5.92
edges	31381	3721	8.43
vertices	20303	3730	5.44
time	9.82	0.05	196.4

Results of comparison of our algorithm with the algorithms described in these works, are given in tables 1 and 2. Quality of the derived continuous skeletons is shown on examples in Fig. 9, 10.

The running time of our algorithm was estimated using Intel processor 1.6 GHz with 512 Mb of memory. Time in tables is specified in seconds.

Comparison with algorithm (Ogniewicz, Kubler, 1995) shows, that using MPP for image boundary approximation allows to reduce dimension of the problem substantially: number of elements in a polygonal figure skeleton is about 6-8 times less than in a corresponding Voronoi diagram of image boundary points. The reduction in computation time (in 196 times) is partially due to this dimension reduction, and partially due to processors capacity increase as compared with SPARCstation-2.

Table 2: Comparison of our algorithm CS and algorithm ST (Strzodka and Telea, 2004).

	Size	ST	CS	ST/CS
Leaf1	410×440=182040	0.14	0.02	70
Room	413×506=208978	0.64	0.03	21
Neuron	839×731=613309	2.5	0.1	25
Roots	1800×1810=3258000	3.79	0.41	9.22

A new parallel discrete skeletonization algorithm is described in Strzodka and Telea (2004). Authors show that the running time of this algorithm is a record for discrete algorithms so far. The table shows the results attained by the authors on GPU GeForce FX 5800 Ultra chip, containing tens independent computers working in a parallel mode. However, it is apparent from table 2, the running time of our algorithm is less than of that algorithm by 1-2 orders. It is necessary to note, that our algorithm can be parallelized too and its operation speed on multicore processors will grow.

5 CONCLUSIONS

The continuous approach to image skeleton construction exceeds in many criteria traditionally applied discrete methods.

1. The continuous skeleton is described by the strict mathematical model. The discrete skeleton doesn't have such strict description; it is validated only as an analogue of a continuous skeleton.

2. Regularization of continuous skeletons, directed on noise overcoming, can be performed by strict mathematical methods; and as for discrete skeletons, it is done on the basis of heuristic devises.

3. The continuous skeleton with the radius function gives more ample opportunities on shape transformations of an object. Comparison of continuous skeletons is reduced to a problem of planar graphs comparison by topological and metric criteria.

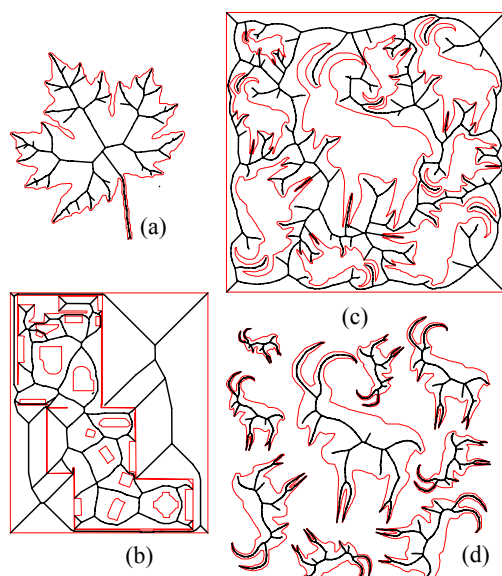


Figure 9: Continuous skeletons: (a) leaf1, (b) room, (c) Billygoat (external), (d) Billygoat (internal).

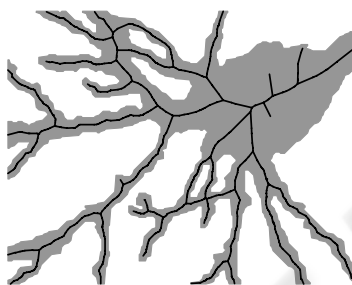


Figure 10: The fragment of the skeleton for "neuron".

4. Running time of continuous skeletonization algorithm is less by at least an order than that of the best samples of discrete skeletonization algorithms.

The downside of application of continuous skeleton construction algorithm is the complexity of its software implementation which demands rather refined programming technique.

ACKNOWLEDGEMENTS

The authors thank Dr. R.Strzodka who has granted us image samples for experiments. Also authors are grateful to the Russian Foundation of Basic Research, which has supported this work (grant 05-01-00542).

REFERENCES

- Bai, X., Latecki, L.J., Liu, W.-Y., 2007. Skeleton pruning by contour partitioning with discrete curve evolution. *IEEE transactions on pattern analysis and machine intelligence*, vol. 29, No. 3, March 2007.
- Blum, H., 1967. A transformation for extracting new descriptors of shape. In *Proc. Symposium Models for the perception of speech and visual form*, MIT Press Cambridge MA, 1967.
- Costa, L., Cesar, R., 2001. *Shape analysis and classification*, CRC Press.
- Deng, W., Iyengar, S., Brener, N., 2000. A fast parallel thinning algorithm for the binary image skeletonization. *The International Journal of High Performance Computing Applications*, 14, No. 1, Spring 2000, pp. 65-81.
- Fortune S., 1987. A sweepline algorithm for Voronoi diagrams. *Algorithmica*, 2 (1987), pp. 153-174.
- Klein, R., Lingas, A., 1995. Fast skeleton construction. In *Proc. 3rd Europ. Symp. on Alg. (ESA'95)*, 1995.
- Lagno, D., Sobolev, A., 2001. Модифицированные алгоритмы Форчуна и Ли скелетизации многоугольной фигуры. In *Graphicon'2001, International Conference on computer graphics, Moscow, 2001* (in Russian).
- Lee, D., 1982. Medial axis transformation of a planar shape. *IEEE Trans. Pat. Anal. Mach. Int.* PAMI-4(4): 363-369, 1982.
- Manzanera, A., Bernard, T., Preteux, F., Longuet, B., 1999. Ultra-fast skeleton based on an isotropic fully parallel algorithm. *Proc. of Discrete Geometry for Computer Imagery*, 1999.
- Mestetskiy, L., 1998. Continuous skeleton of binary raster bitmap. In *Graphicon'98, International Conference on computer graphics, Moscow, 1998* (in Russian).
- Mestetskiy, L., 2000. Fat curves and representation of planar figures. *Computers & Graphics*, vol.24, No. 1, 2000, pp.9-21.
- Mestetskiy, L., 2006. Skeletonization of a multiply connected polygonal domain based on its boundary adjacent tree. In *Siberian journal of numerical mathematics*, vol.9, N 3, 2006, 299-314, (in Russian).
- Ogniewicz, R., Kubler, O., 1995. Hierarchic Voronoi Skeletons. *Pattern Recognition*, vol. 28, no. 3, pp. 343-359, 1995.
- Smith R., 1987. Computer processing of line images: A survey. *Pattern recognition*, vol. 20, no.1, pp.7-15, 1987.
- Srinivasan, V., Nackman, L., Tang, J., Meshkat, S., 1992. Automatic mesh generation using the symmetric axis transform of polygonal domains, *Proc. of the IEEE*, 80 (9) (1992), pp. 1485-1501.
- Strzodka, R., Telea, A., 2004. Generalized Distance Transforms and Skeletons in Graphics Hardware. *Joint EUROGRAPHICS - IEEE TCVG Symposium on Visualization (2004)*.
- Yap C., 1987. An $O(n \log n)$ algorithm for the Voronoi diagram of the set of simple curve segments. *Discrete Comput. Geom.*, 2(1987), pp. 365-393.